

ChemComm

Accepted Manuscript



This article can be cited before page numbers have been issued, to do this please use: Y. Liu, H. Ma, L. Zhang, Y. Cui, X. Liu and J. Fang, *Chem. Commun.*, 2015, DOI: 10.1039/C5CC09998F.



This is an *Accepted Manuscript*, which has been through the Royal Society of Chemistry peer review process and has been accepted for publication.

Accepted Manuscripts are published online shortly after acceptance, before technical editing, formatting and proof reading. Using this free service, authors can make their results available to the community, in citable form, before we publish the edited article. We will replace this *Accepted Manuscript* with the edited and formatted *Advance Article* as soon as it is available.

You can find more information about *Accepted Manuscripts* in the [Information for Authors](#).

Please note that technical editing may introduce minor changes to the text and/or graphics, which may alter content. The journal's standard [Terms & Conditions](#) and the [Ethical guidelines](#) still apply. In no event shall the Royal Society of Chemistry be held responsible for any errors or omissions in this *Accepted Manuscript* or any consequences arising from the use of any information it contains.



Journal Name

A Small Molecule Probe Reveals Declined Mitochondrial Thioredoxin Reductase Activity in a Parkinson's Disease Model

Received 00th January 20xx,
Accepted 00th January 20xx

Yaping Liu, Huilong Ma, Liangwei Zhang, Yajing Cui, Xiaoting Liu, and Jianguo Fang*

DOI: 10.1039/x0xx00000x

www.rsc.org/

The first off-on probe, Mito-TRFS, for imaging the mitochondrial thioredoxin reductase (TrxR2) in live cells was reported. In a cellular model of Parkinson's disease (PD), Mito-TRFS staining discloses a drastic decline of the TrxR2 activity, providing a mechanistic link of TrxR2 dysfunction to the etiology of PD.

Thioredoxin reductases (TrxRs) are members of the pyridine nucleotide-disulfide oxidoreductase family and are ubiquitously found in all living cells. Two major isoforms of TrxRs are present in different intracellular organelles: TrxR1 is predominantly in the cytosol and nucleus, while TrxR2 is mainly localized within mitochondria.¹⁻³ A third form, thioredoxin and glutathione reductase (TrxR3), is mainly expressed in testis.⁴ Despite the different localizations of the isoforms within cells, mammalian TrxRs have similar structures with a conserved selenocysteine (Sec) residue at the C-terminus and share the same catalytic mechanism. TrxRs play key roles in regulating diverse redox-mediated cellular events, including gene transcription, DNA/protein damage recognition and repair, cell proliferation, and apoptosis.^{3, 5} The malfunction of TrxRs has been implicated in various diseases, such as cardiovascular diseases, inflammation, neurodegenerative diseases, and cancer.^{6, 7}

Reactive oxygen species (ROS) are constantly produced from numerous cellular processes. ROS at low levels may act as signaling molecules to activate cellular proliferation and survival pathways. However, ROS at high levels lead to oxidative stress and ultimately cause cell death.^{8, 9} Mitochondria are major sites for ROS production, and may produce up to 90% of cellular ROS.¹⁰ Although mitochondrial dysfunction is implicated in the etiology of various neurodegenerative diseases including Parkinson's disease (PD), the underlying molecular mechanisms are not well defined. TrxR2, together with its substrate thioredoxin 2 (Trx2), is a leading player to direct or interact with other antioxidant molecules, such as peroxiredoxin 3, to control ROS levels in mitochondria.^{5, 11} Thus, monitoring TrxR2 activity is of physiological significance to better understand its role in cellular redox regulation. We previously reported the first selective off-on TrxRs fluorescent probe, TRFS-green.¹² TRFS-green can readily image the TrxRs activity in various

types of live cells.¹³⁻¹⁷ However, this probe is not suitable for specific TrxR2 imaging as TRFS-green appears evenly distributed in cytosol. Detection of TrxR2 activity in cells is tedious. Prior to the assay, cells have to be broken to isolate mitochondria. Then the total mitochondrial proteins are extracted and the activity of TrxR2 in the extracts is determined by the classic thioredoxin-mediated insulin reduction assay.^{2, 18-21} This time- and labor-consuming determination of TrxR2 hampers the study of the physiological functions of the mitochondrial enzyme. Herein, we reported the synthesis of a mitochondria-targeted TrxR probe, Mito-TRFS, and evaluation of the probe in vitro and in live cells. Our results indicated that Mito-TRFS accumulated exclusively in mitochondria and could image TrxR2 activity specifically in live cells. More importantly, in the 6-hydroxydopamine (6-OHDA)-treated PC12 cells, a well-established cellular model of PD, the TrxR2 activity was drastically declined revealed by Mito-TRFS staining, which provides a mechanistic link of TrxR2 malfunction to PD.

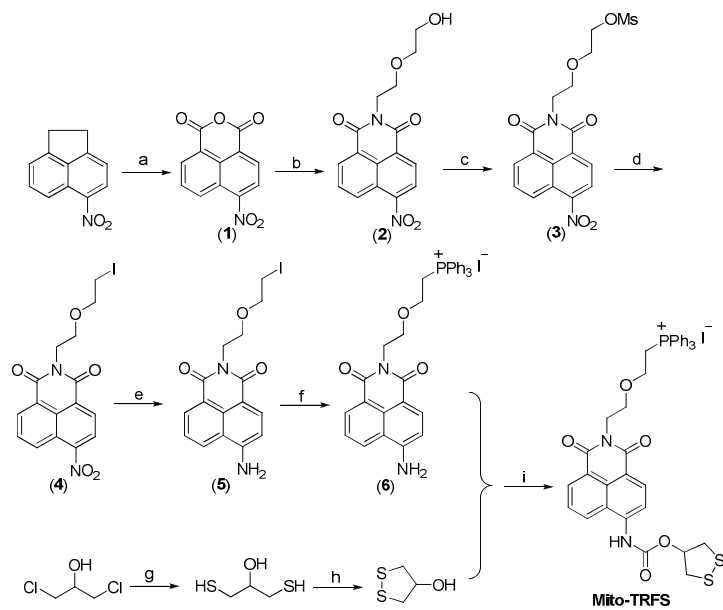
We incorporated the triphenylphosphonium moiety, a well-documented mitochondria-targeting motif,²²⁻²⁹ into the parent molecule TRFS-green, and generated the selective TrxR2 probe Mito-TRFS, whose synthetic routes were outlined in Scheme 1. The fluorophore naphthalimide (**6**) was synthesized in six steps (steps a-f) with the overall yield of 7.8 % from the readily available acenaphthene by adapting the published procedures.^{23, 30, 31} The TrxR-recognizing part, 1, 2-dithiolan-4-ol (**8**), was synthesized in two steps (steps g & h) with the overall yield of 52 % from the commercially available 1, 3-dichloropropan-2-ol by following previously published procedures.¹² For the synthesis of Mito-TRFS, **6** was reacted with diphosgene in the presence of N, N-diisopropylethylamine (DIPEA) in dichloromethane (DCM), followed by the addition of **2**. After purification by silica gel column chromatography, Mito-TRFS was obtained in 10 % yield. The chemical structures of Mito-TRFS and the synthetic intermediates were characterized by ¹H NMR, ¹³C NMR and MS. The original spectra were included in the Supporting Information (Figures S3-22).

State Key Laboratory of Applied Organic Chemistry and College of Chemistry and Chemical Engineering, Lanzhou University, Lanzhou 730000, China.

* Corresponding author, E-mail: fangjg@lzu.edu.cn

Electronic Supplementary Information (ESI) available: Experimental details, original NMR and MS spectra and supplementary figure]. See DOI: 10.1039/x0xx00000x

Journal Name



Scheme 1 Synthesis of Mito-TRFS. Reagents and conditions: (a) $\text{Na}_2\text{Cr}_2\text{O}_7/\text{AcOH}$, reflux, 76 %; (b) 2-(2-aminoethoxy)ethanol/THF, reflux, 50 %; (c) $\text{MsCl}/\text{Et}_3\text{N}/\text{DCM}$, r. t., 55 %; (d) $\text{NaI}/\text{acetone}$, 80 %; (e) $\text{SnCl}_2 \cdot 2\text{H}_2\text{O}/\text{HCl}/\text{EtOH}$, reflux, 58 %; (f) PPh_3/MeCN , 80 %; (g) $\text{Na}_2\text{S}/\text{CS}_2$, 60 °C, 59 %; (h) $\text{NaHCO}_3/\text{I}_2/\text{DCM}$, r. t., 89 %; (i) diphosgene/DIPEA/DCM, reflux, 10 %.

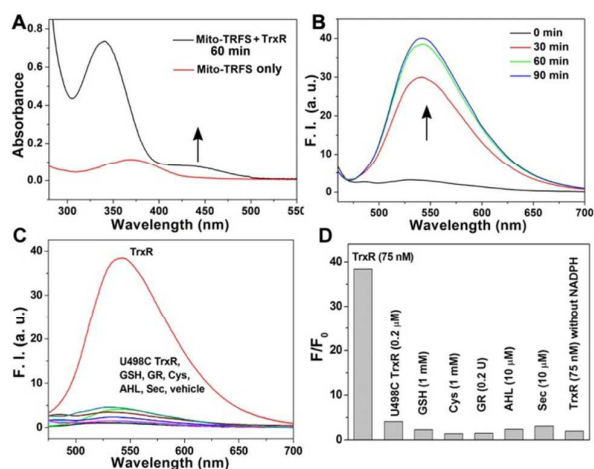


Fig. 1 Response of Mito-TRFS to TrxR. Absorption spectra (A) and Fluorescence spectra ($\lambda_{\text{ex}}=438$ nm, B) of Mito-TRFS with or without TrxR and NADPH. The arrows in (A) & (B) show the change of absorbance at 438 nm and emission at 540 nm, respectively. (C) Selective recognition of Mito-TRFS by TrxR. The spectra ($\lambda_{\text{ex}}=438$ nm) were acquired after the probe was incubated with GSH, Cys, various enzymes (TrxR, U498C TrxR, and GR) with NADPH (200 μM), AHL (10 μM) or Sec (10 μM) at 37 °C for 60 min. (D) The fold of fluorescence increment (F/F_0) from (C) was shown.

Initially, we examined the absorption and emission spectra of Mito-TRFS in responding to the TrxR (Figure 1). Mito-TRFS (10 μM) has the maximal absorption at ~ 375 nm in TE buffer (50 mM Tris-HCl and 1 mM EDTA, pH 7.4) at 37 °C. After addition of the recombinant rat TrxR1 (75 nM) and NADPH (200 μM), its maximum absorbance is red-shifted to ~ 438 nm (Figure 1A). The strong absorbance at ~ 340 nm in Figure 1A was from NADPH. Mito-TRFS itself has a strong emission at ~ 480 nm when excited at 375 nm in TE buffer ($\phi=0.34$), but has weak emission when excited at 438 nm. However, the emission centered at ~ 540 nm increases remarkably after addition of the TrxR1 and NADPH (Figure 1B, $\phi=0.19$). The increment of the fluorescence intensity reaches a plateau after 60 min. Mito-TRFS displayed faster response to TrxR compared to its parent molecule TRFS-green: The fluorescence increment of Mito-TRFS triggered by TrxR is about 30-fold within 60 min while that for TRFS-green is about 25-fold within 3 h.¹² We reasoned that this could be due to that Mito-TRFS is more hydrophilic than TRFS-green. Furthermore, Mito-TRFS bears a positive charge, which facilitates its binding to the negative-charged C-terminal active site of TrxR via the electrostatic interaction. These might contribute to the faster response of Mito-TRFS than TRFS-green.

We next determined whether Mito-TRFS (10 μM) could be selectively triggered on by TrxR. As shown in Figures 1C & 1D, neither GSH nor Cys causes significant increment of the fluorescence signal. The glutathione reductase (GR), whose structure is closely related to TrxR, has little effect on the reduction of Mito-TRFS. Furthermore, the U498C TrxR, where the Sec498 was

replaced by Cys, also displays negligible interference of the emission signal, supporting the critical role of the Sec residue of the enzyme to turn on the fluorescence. Amidehydrolase (AHL), Sec, and TrxR without NADPH also give marginal response to the probe. The Sec (10 μM) was generated in situ by mixing Cys (1 mM) and selenocysteine (5 μM), and the presence of the selenol group was confirmed by our specific selenol probe Sel-green.³² Taken together, Mito-TRFS maintains the high selectivity to TrxR. This is not surprising as the recognition part of Mito-TRFS is the same as that of specific TrxR probe TRFS-green.¹² Introduction of the triphenylphosphonium moiety would facilitate the probe to restrict in mitochondria.

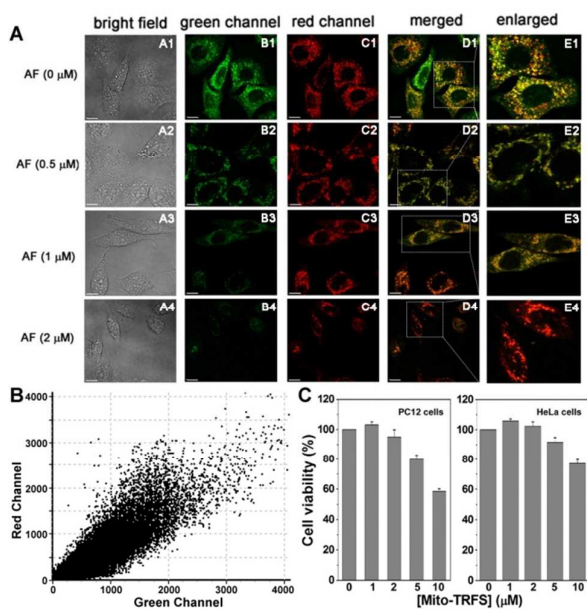


Fig. 2 Confocal fluorescence images of HeLa cells. The cells were incubated with vehicle (0.1 % DMSO, A1-E1) or varying concentrations of AF (A2-E4) for 4 h followed by further treated with Mito-TRFS (1 μM) for 2 h. Then, the cells were stained with MTD R (100 nM) for 15 min. Scale bars: 10 μm . (B) Scatter plot of colocalization events as shown in E1 panel. (C) Cytotoxicity of Mito-TRFS to PC12 and HeLa cells after 24 h treatment.

We then conducted a fluorescence colocalization assay to ensure that the probe localizes exclusively in mitochondria (Figure 2). Upon selective excitation at 458 nm, the cells exhibited bright green fluorescence in discrete subcellular distribution as determined by laser confocal microscopy (B1). The image from MTD R-staining was obtained upon selective excitation at 633 nm and emission collection from 650 to 740 nm (C1). The merge of B1 and C1 gives a clear colocalization signal as the yellow color (D1) with a colocalization coefficient of 0.90 (Figure 2B), confirming that Mito-TRFS is localized predominantly in the mitochondria of live cells. The highlighted part in the merged picture was enlarged in E1. The pictures in the panels B2, B3, & B4 show dose-dependent inhibition of the green fluorescence signal after the cells were

pretreated with the specific TrxR inhibitor auranofin (AF) for 6 h, indicating a selective recognition of TrxR by Mito-TRFS. There is no significant toxicity of Mito-TRFS (<2 μM) to the cultured cells (Figure 2C). Taken together, our results demonstrate that Mito-TRFS is suitable for selective imaging of mitochondrial TrxR in live cells.

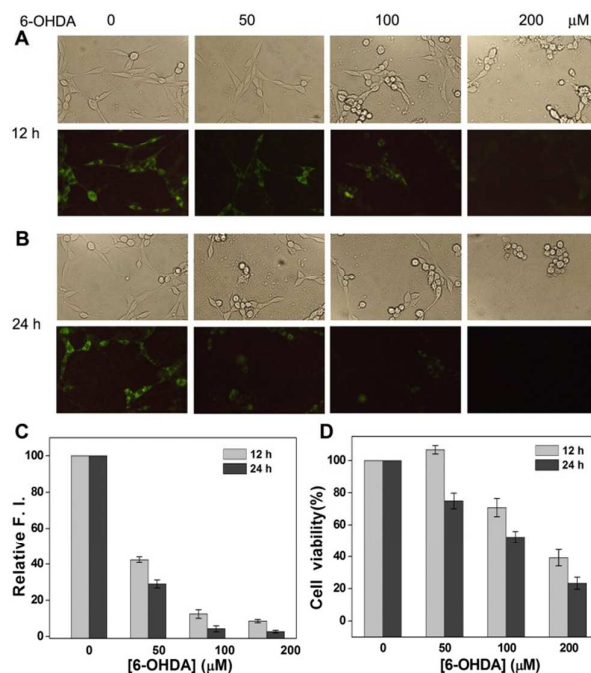


Fig. 3 Decline of TrxR2 activity in the PD model. PC12 cells were treated with 6-OHDA for 10 h (A) or 22 h (B). Mito-TRFS (1 μM) was added and continued incubation for 2 h. The cells were photographed under a Leica inverted fluorescence microscope. (C) Relative fluorescence intensity in individual cells from (A) and (B) were quantified by a flow cytometer. (D) Cytotoxicity of 6-OHDA to PC 12 cells. Data were expressed as the mean \pm SD from duplicates.

Mitochondrial ROS play important roles in physiological signaling.³³ However, uncontrolled ROS production contributes to the pathological degeneration of neurons associated with neurodegenerative diseases such as PD.^{34, 35} As major sites for ROS generation, mitochondria have evolved multiple antioxidant pathways to help maintaining the balance between ROS production and removal. TrxR2 is a mitochondria-located antioxidant enzyme to serve as a relay to transfer electrons from NADPH to its substrate Trx2, which interacts with diverse downstream substrates to regulate the redox homeostasis of mitochondria.¹¹ Although the dysfunction of TrxR2 has been suggested to link to the PD, the direct evidence is limited presumably due to the inconvenient assay of TrxR2. There is no direct probe to detect the TrxR2 activity in live cells prior to this study. We presented evidence here that TrxR2 activity is severely impaired in a cellular model of PD. 6-OHDA is widely used in generating cell or animal models of PD.³⁶⁻³⁸ We treated the neuron-like PC12 cells with the neurotoxin 6-OHDA to generate the PD model, and then determined the TrxR2 activity by Mito-TRFS staining. As shown in Figures 3A & 3B, 6-OHDA

COMMUNICATION

Journal Name

treatment causes both dose- and time-dependent suppression of the fluorescence. The majority of the cells were alive when they were treated with 50 μM or 100 μM 6-OHDA (Figure 3D). However, the TrxR2 activity was significantly inhibited evidenced by the fluorescence imaging. The concentrations of 6-OHDA used in the experiments, ranging from 50-200 μM , cover the most concentrations used for generating cellular model of PD in the literature. This is the first observation of TrxR2 dysfunction in PD model in live cells, thus providing a mechanistic link of TrxR2 dysfunction to the occurrence of PD. The relative fluorescence intensity in individual cells was further quantified by flow cytometry analysis (Figure 3C & Figures S1 & S2). 6-OHDA appears targeting the mitochondria preferably, and its neurotoxicity is thought to be mediated by the redox cycling to generate ROS and electrophilic quinone intermediates,^{37, 39} both of which could readily inhibit TrxR2 within the mitochondrial compartment. This might account for the severe inhibition of TrxR2 in the 6-OHDA-treated PC12 cells. There is no significant alteration of the TrxR2 expression in PC12 cells after 6-OHDA challenge (Figure S23), suggesting that the decline of the enzyme activity is due to the inhibition of the enzyme by 6-OHDA or its metabolites.

In conclusion, Mito-TRFS, the first turn-on probe for mitochondrial TrxR, was prepared and evaluated. The probe exhibits highly selectivity to image the TrxR2 activity in live cells. Furthermore, with the aid of Mito-TRFS, we disclosed that the severe suppression of TrxR2 activity in a model of PD, providing a mechanistic link between TrxR2 dysfunction and the etiology of PD. We expect that Mito-TRFS would be a powerful tool to dissect the physiological/pathological functions of TrxR2 in living systems.

ACKNOWLEDGEMENTS

The financial supports from Natural Science Foundation of China (21572093) and Natural Science Foundation of Gansu Province (145RJZA225) are acknowledged. The authors also express appreciation to Prof. Arne Holmgren (Karolinska Institute, Sweden) for the recombinant rat TrxR1. There are no conflicts of interest.

Notes and references

- W. Cai, L. Zhang, Y. Song, B. Wang, B. Zhang, X. Cui, G. Hu, Y. Liu, J. Wu and J. Fang, *Free Radic. Biol. Med.*, 2012, **52**, 257.
- M. P. Rigobello and A. Bindoli, *Methods Enzymol.*, 2010, **474**, 109.
- E. S. Arner, *Biochim. Biophys. Acta*, 2009, **1790**, 495.
- Q. A. Sun, L. Kirnarsky, S. Sherman and V. N. Gladyshev, *Proc. Natl. Acad. Sci. U S A*, 2001, **98**, 3673.
- J. Lu and A. Holmgren, *Free Radic. Biol. Med.*, 2014, **66**, 75.
- D. F. Mahmood, A. Abderrazak, E. H. Khadija, T. Simmet and M. Rouis, *Antioxid. Redox Signal.*, 2013, **19**, 1266.
- A. Holmgren and J. Lu, *Biochem. Biophys. Res. Commun.*, 2010, **396**, 120.
- M. Schieber and N. S. Chandel, *Curr. Biol.*, 2014, **24**, R453.
- B. D'Autreaux and M. B. Toledano, *Nat. Rev. Mol. Cell Biol.*, 2007, **8**, 813.
- R. S. Balaban, S. Nemoto and T. Finkel, *Cell*, 2005, **120**, 483.
- A. Miranda-Vizuete, A. E. Damdimopoulos and G. Spyrou, *Antioxid. Redox Signal.*, 2000, **2**, 801.
- L. Zhang, D. Duan, Y. Liu, C. Ge, X. Cui, J. Sun and J. Fang, *J. Am. Chem. Soc.*, 2014, **136**, 226.
- B. Zhang, D. Duan, C. Ge, J. Yao, Y. Liu, X. Li and J. Fang, *J. Med. Chem.*, 2015, **58**, 1795.
- S. Peng, B. Zhang, J. Yao, D. Duan and J. Fang, *Food Funct.*, 2015, **6**, 2091.
- S. Peng, B. Zhang, X. Meng, J. Yao and J. Fang, *J. Med. Chem.*, 2015, **58**, 5242.
- S. Peng, J. Yao, Y. Liu, D. Duan, X. Zhang and J. Fang, *Food Funct.*, 2015, **6**, 2813.
- Y. Liu, D. Duan, J. Yao, B. Zhang, S. Peng, H. Ma, Y. Song and J. Fang, *J. Med. Chem.*, 2014, **57**, 5203.
- P. Lopert and M. Patel, *J. Biol. Chem.*, 2014, **289**, 15611.
- V. Branco, A. Godinho-Santos, J. Goncalves, J. Lu, A. Holmgren and C. Carvalho, *Free Radic. Biol. Med.*, 2014, **73**, 95.
- M. P. Rigobello, G. Scutari, A. Folda and A. Bindoli, *Biochem. Pharmacol.*, 2004, **67**, 689.
- I. Nalvarte, A. E. Damdimopoulos and G. Spyrou, *Free Radic. Biol. Med.*, 2004, **36**, 1270.
- J. Zhou, L. Li, W. Shi, X. Gao, X. Li and H. Ma, *Chem. Sci.*, 2015, **6**, 4884.
- L. Yuan, L. Wang, B. K. Agrawalla, S. J. Park, H. Zhu, B. Sivaraman, J. Peng, Q. H. Xu and Y. T. Chang, *J. Am. Chem. Soc.*, 2015, **137**, 5930.
- H. S. Jung, J. Han, J. H. Lee, J. M. Choi, H. S. Kweon, J. H. Han, J. H. Kim, K. M. Byun, J. H. Jung, C. Kang and J. S. Kim, *J. Am. Chem. Soc.*, 2015, **137**, 3017.
- M. H. Lee, N. Park, C. Yi, J. H. Han, J. H. Hong, K. P. Kim, D. H. Kang, J. L. Sessler, C. Kang and J. S. Kim, *J. Am. Chem. Soc.*, 2014, **136**, 14136.
- Q. Hu, M. Gao, G. Feng and B. Liu, *Angew. Chem. Int. Ed. Engl.*, 2014, **53**, 14225.
- H. Yuan, H. Cho, H. H. Chen, M. Panagia, D. E. Sosnovik and L. Josephson, *Chem. Commun.*, 2013, **49**, 10361.
- M. H. Lee, J. H. Han, J. H. Lee, H. G. Choi, C. Kang and J. S. Kim, *J. Am. Chem. Soc.*, 2012, **134**, 17314.
- M. P. Murphy and R. A. Smith, *Annu. Rev. Pharmacol. Toxicol.*, 2007, **47**, 629.
- B. Zhang, C. Ge, J. Yao, Y. Liu, H. Xie and J. Fang, *J. Am. Chem. Soc.*, 2015, **137**, 757.
- V. Percec, E. Aqad, M. Peterca, M. R. Imam, M. Glodde, T. K. Bera, Y. Miura, V. S. Balagurusamy, P. C. Ewbank, F. Wurthner and P. A. Heiney, *Chem. Eur. J.*, 2007, **13**, 3330.
- B. Zhang, C. Ge, J. Yao, Y. Liu, H. Xie and J. Fang, *J. Am. Chem. Soc.*, 2015, **137**, 757.
- Y. Collins, E. T. Chouchani, A. M. James, K. E. Menger, H. M. Cocheme and M. P. Murphy, *J. Cell Sci.*, 2012, **125**, 801.
- M. T. Lin and M. F. Beal, *Nature*, 2006, **443**, 787.
- P. C. Trippier, K. Jansen Labby, D. D. Hawker, J. J. Mataka and R. B. Silverman, *J. Med. Chem.*, 2013, **56**, 3121.
- N. Simola, M. Morelli and A. R. Carta, *Neurotox. Res.*, 2007, **11**, 151.
- Y. Saito, K. Nishio, Y. Ogawa, T. Kinumi, Y. Yoshida, Y. Masuo and E. Niki, *Free Radic. Biol. Med.*, 2007, **42**, 675.
- L. Li, C. W. Zhang, J. Ge, L. Qian, B. H. Chai, Q. Zhu, J. S. Lee, K. L. Lim and S. Q. Yao, *Angew. Chem. Int. Ed. Engl.*, 2015, **54**, 10821.
- S. Eminel, A. Klettner, L. Roemer, T. Herdegen and V. Waetzig, *J. Biol. Chem.*, 2004, **279**, 55385.

Journal Name COMMUNICATION

TOC

